NANO LETTERS

2003
Vol. 3, No. 2
157−161

Efficient Formation of Iron Nanoparticle Catalysts on Silicon Oxide by Hydroxylamine for Carbon Nanotube Synthesis and Electronics

Hee Cheul Choi, Summit Kundaria, Dunwei Wang, Ali Javey, Qian Wang, Marco Rolandi, and Hongjie Dai*

Department of Chemistry, Stanford University, Stanford, California 94305

Received November 2, 2002; Revised Manuscript Received November 25, 2002

ABSTRACT

Iron containing nanoparticles are found to spontaneously form on hydroxylated SiO_2 substrates when immersed in a freshly mixed aqueous solution of $FeCl_3$ and hydroxylamine. Upon calcination, a submonolayer of uniformly distributed iron oxide nanoparticles can be derived and used to catalyze the growth of single-walled carbon nanotubes by chemical vapor deposition. This simple method affords clean single-walled nanotube films on SiO_2. The solution phase catalyst deposition approach allows for submicron scale catalyst patterning. Patterned growth of nanotubes with this catalyst retains high degrees of surface cleanliness and leads to arrays of nanotube electronic devices including field effect transistors. The population of hydroxyl groups on SiO_2, reaction time, and pH of the solutions are found to be important to the deposition of nanoparticles through a surface-mediated hydroxylamine/$FeCl_3$ chemistry.

Introduction. Chemical vapor deposition (CVD) of single-walled carbon nanotubes (SWNT) on substrates is a promising approach to organized molecular wire structures.[1] Patterned growth assisted by self-assembly and electric-field directed assembly produces site-specific and oriented nanotube arrays,[2−6] useful for device integration without post-growth nanotube purification and assembly.[7−10] Lying at the heart of nanotube CVD is catalytic nanoparticles. It is essential to develop novel methods for catalyst nanoparticle formation, and their delivery and patterning on substrates.[1] Patterned growth of SWNTs at the level of a few microns was initially demonstrated with Fe catalyst supported on aluminum oxide powders.[2] While clean SWNTs emanating from catalytic sites were readily obtained, the catalytic regions on the substrate were not clean. Mound-like patterned alumina particles could cause problems to characterizations by, for example, atomic force microscopy (AFM), as the imaging tip frequently picked up these particles. Catalysts supported on powders are also less desired for individual catalytic nanoparticle size control and patterning of nanoparticles at smaller scales (e.g., $< 1\ \mu m$). Progress has been made recently in creating size-controlled discrete catalyst nanoparticles on flat substrates for SWNT growth.[11−13] We have formed catalytic nanoparticles with appoferritin[11] and PAMAM dendrimer[13] hosts for growth of SWNTs with diameters in the range of 1−2 nm. Cheung and co-workers used catalyst nanoparticles derived in organic solvents for the synthesis of SWNTs with 3−12 nm diameters.[12] Deposition and patterning of solution-derived discrete nanoparticles allows for patterned growth of nanotubes with clean substrate surfaces.[14]

Here, we report a simple approach to the formation of Fe containing catalyst nanoparticles (up to a monolayer) on SiO_2 wafers for CVD synthesis of SWNTs. We find that simple soaking of SiO_2 wafers in a freshly mixed aqueous solution of hydroxylamine and $FeCl_3$ leads to spontaneous deposition of nanoparticles on the substrates. The nanoparticles are then fully converted to Fe_2O_3 and used to catalyze SWNT growth. The solution phase catalyst deposition approach allows for submicron scale patterned nanotube growth that retains a high degree of surface cleanliness, which facilitates characterization and device fabrication of, for example, nanotube field effect transistors (FETs). Hydroxylamine is known as a mild reducing agent and has been previously used to reduce $AuCl_4^-$ ions on surface-supported Au nanoparticles for enlarging the particles.[15] In our system, deposition of Fe-containing nanoparticles on SiO_2 substrates from the hydroxylamine and $FeCl_3$ solution appears to be mediated by the hydroxyl groups on SiO_2. The reaction time and pH of the solution is found to determine the size and density of the nanoparticles.

Experimental Section. 500 nm thick SiO_2 layers were grown on p-type Si wafers by oxidation at 1000 °C in a wet

* Corresponding author. E-mail hdai@stanford.edu.

10.1021/nl025876d CCC: $25.00
Published on Web 12/17/2002

environment (with H_2 and O_2 at a ratio of 150:1000 in the thermal oxidation chamber). The substrates were cleaned with copious amounts of acetone, methanol, and 2-propanol and then dried under a N_2 stream prior to use. $FeCl_3 \cdot 6H_2O$, hydroxylamine hydrochloride ($NH_2OH \cdot HCl$), and double-distilled water were used as received (Aldrich). The Fe-containing nanoparticle formation was achieved by immersing the SiO_2 substrate into a scintillation vial containing 10 mL of water and 10 μL of 10 mM $FeCl_3 \cdot 6H_2O$(aq), followed by immediate addition of 100 μL of 40 mM $NH_2OH \cdot HCl$(aq) into the vial. The concentrations of Fe(III) and hydroxylamine in the reaction solution (pH = 4.8) were 10 μM and 400 μM, respectively. After a few seconds stirring, the substrate was allowed to soak in the solution for a certain period of time (10 s to 5 min) before being taken out of the solution, rinsed consecutively with water, acetone, and isopropyl alcohol, and dried.

Note that a fresh aqueous $FeCl_3 \cdot 6H_2O$ stock solution was prepared daily to avoid formation of aggregates in the solution. After this solution phase deposition process, the substrate was calcined in air at 800 °C for 5 min, followed by CVD growth on the substrate at 900 °C for 10 min in a 1" tube furnace under combined flows of 1000 sccm of CH_4, 500 sccm of H_2, and 20 sccm of C_2H_4.[14] During the heating process, the carrier gas (H_2) was switched to the reacting gases when the temperature of the furnace reached 830 °C and then ramped up to 900 °C.

An atomic force microscope operating in the tapping mode (Digital Instruments) was used to image the substrate after solution phase deposition, calcination, and CVD synthesis. Imaging by scanning electron microscopy (SEM, FEI, operating voltage 5 kV) and transmission electron microscopy (TEM, Philips CM20, 200 kV) were also carried out. For TEM, SWNTs were directly synthesized on thin SiO_2 films (10 nm thick, transparent to electron beams[11,16]) on TEM grids (Ted Pella, Inc.). Micro-Raman spectroscopy (Renishaw 1000) was used to characterize the SWNTs grown on SiO_2. The excitation wavelength was 788 nm (1.58 eV) sourced by an AlGaAs diode laser with a spot size of ~1 μm.

Results and Discussion. Figure 1a shows an AFM image of a SiO_2 substrate after soaking in the hydroxylamine/$FeCl_3$ solution for 2 min. While the original SiO_2 surface prior to the solution treatment was very smooth with a root-mean-square surface roughness of ~0.2 nm (Figure 1a, inset), 2 min soaking in the hydroxylamine/$FeCl_3$ solution led to the formation of close to a monolayer of nanoparticles on the substrate (Figure 1a). The average height of the nanoparticles was ~2.2 ± 0.9 nm (with a very small percentage of the particles up to 6 nm tall). After calcination at 800 °C in air for 5 min, the nanoparticles appeared smaller, with an average height of ~1.5 ± 0.6 nm (Figure 1b) and a similar area density as before calcination. With the nanoparticles thus formed on SiO_2, AFM, SEM, and TEM revealed that SWNTs were produced on the substrate after CVD (Figure 2). AFM (Figure 2a) showed abundant tube-like structures after the synthesis with an average height of ~ 1.6 ± 0.5 nm. The substrates appeared clean without the presence of

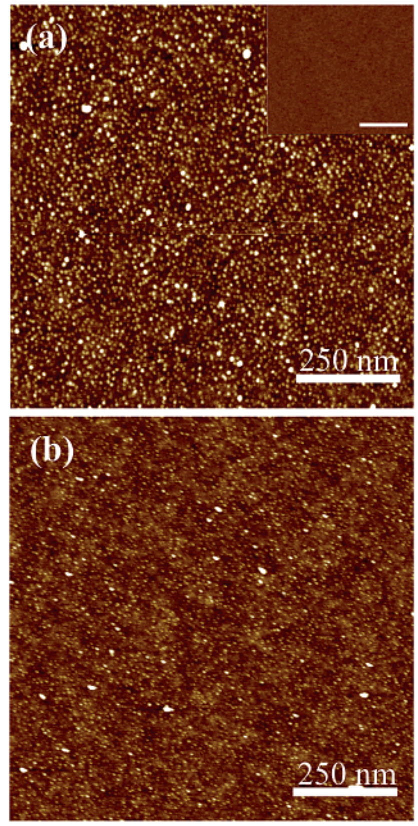

Figure 1. AFM images of (a) nanoparticles formed on SiO_2 after soaking in the hydroxylamine/$FeCl_3$ solution for 2 min and (b) iron-oxide nanoparticles after calcination in air at 800 °C for 5 min, respectively. The inset in (a) shows a bare SiO_2 surface and the scale bar is 1 μm.

large particulates that interfere with AFM imaging. SEM (Figure 2b, operated at a low voltage of 5 kV) revealed nanotubes making a film-like morphology (as grown, without metal coating on sample). The film was clean, smooth, and of high purity without unwanted deposits or impurities. TEM imaging (Figure 2c) confirmed that the nanotubes were single-walled with average diameter of ~1.5 nm, consistent with AFM height data. Note that SWNTs could also be synthesized without the calcination step. Resonant micro-Raman spectroscopy was used to characterize nanotubes in ~1 μm^2 areas on the SiO_2 substrates. A measure of the nanotube diameter (d, in nm) was made from the Raman shift (ω_r, in cm^{-1}) of its radial breathing mode by $d = 248$ cm^{-1} nm/ω_r.[17] Figure 3a shows a typical resonant Raman spectrum acquired with SWNTs grown from the hydroxylamine derived nanoparticles. The two peaks at 158 and 204 cm^{-1} are identified as the radial breathing modes of two SWNTs with diameters of 1.6 and 1.2 nm, respectively. The peak at 1604 cm^{-1} corresponds to one of the in-plane vibrational modes of a graphene sheet centered at 1580 cm^{-1}. Based on about 100 micro-Raman spectra for 164 nanotubes, we find that the diameters of the nanotubes measured this way range from 0.9 to 2.4 nm (Figure 3b).

A set of control experiments has been performed in order to investigate the formation of nanoparticles on SiO_2 upon immersion in the hydroxylamine/$FeCl_3$ solution. When varying the soaking time, we find that the population of

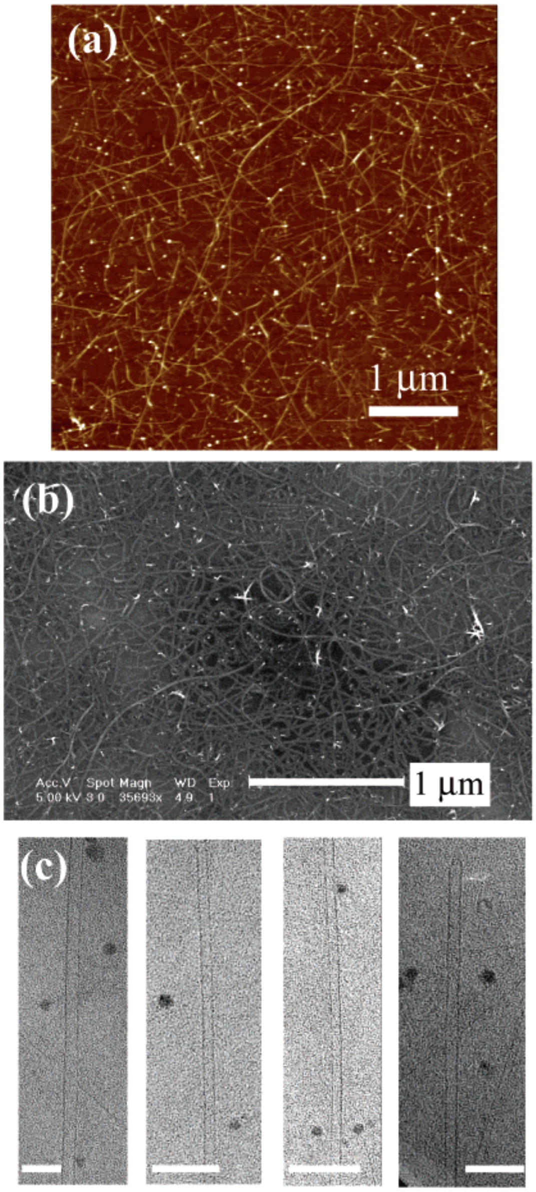

Figure 2. (a) AFM and (b) SEM images of SWNT films grown from a near-monolayer of catalyst nanoparticles on SiO_2 via hydroxylamine assisted deposition. (c) Several TEM images of individual SWNTs grown on SiO_2 TEM grids. The back-ground is the 10 nm thick SiO_2 film and appears somewhat granular. Scale bars: 5 nm.

nanoparticles can vary. The density of deposited particles after 10 s of soaking (Figure 4a) is significantly lower than those after 1 min (Figure 1a) and 5 min (Figure 4b) of soaking conditions. For longer immersion (>10 min), the particles on the substrate appear larger. We have also soaked SiO_2 substrates in a solution without hydroxylamine but with $FeCl_3$ at the same 10 μM concentration. No systematic particle deposition is observed on the substrate except for sparse decorations and occasional regions with higher densities of particles (Figure 4c).

Further control experiments suggest that surface hydroxyl groups on SiO_2 appear to participate in the reaction that leads to the deposition of iron-containing nanoparticles from the hydroxylamine/$FeCl_3$ solution. Substrates used for these

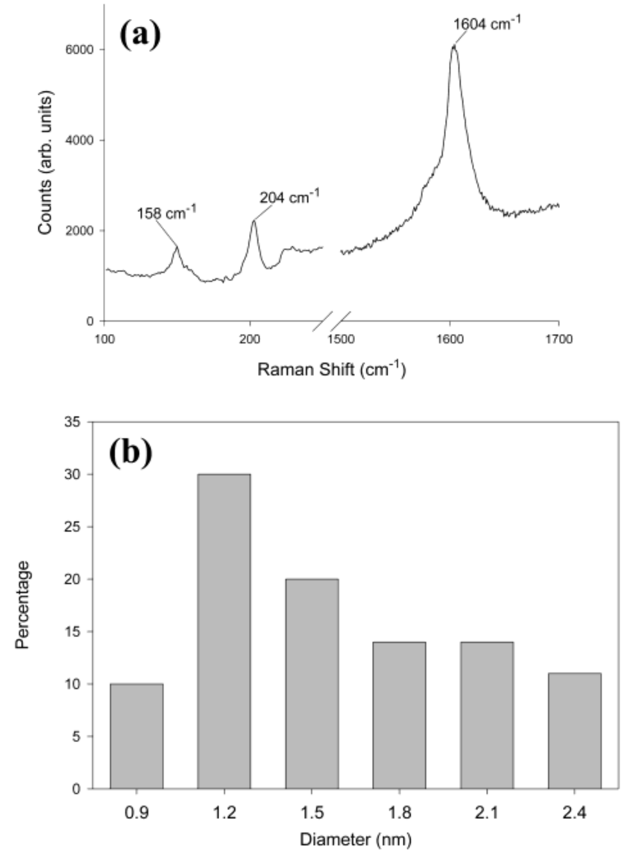

Figure 3. (a) Representative micro-Raman spectroscopy of SWNTs in a 1 μm^2 area of SiO_2. (b) Nanotube diameter distribution measured from resonance micro-Raman data.

experiments include SiO_2 wafers as-made by oxidation in a wet environment, SiO_2 wafers treated in boiling piranha solution at 90 °C, and the thermally grown SiO_2 wafers calcined in ambient air at 800 °C for 10 min. Upon 1 min soaking in hydroxylamine/$FeCl_3$ solutions, the piranha treated SiO_2 exhibit density and morphology of deposited nanoparticles similar to the as-made thermally grown SiO_2. For the SiO_2 wafer calcined in air at 800 °C, much less deposition is observed on the substrate after 1 min soaking in the same solution (Figure 4d) for the same deposition time. The surfaces of our SiO_2 wafers obtained by wet thermal oxidation appear fully hydroxylated, as further treatment in piranha solution does not appear to significantly increase the hydroxyl group density. On the other hand, it is known that high temperature calcination in relatively dry air removes hydroxyl groups via irreversible silanol formation.[18] Hence, our control experiments suggest that a high density of $-OH$ groups on SiO_2 is needed for efficient nanoparticle deposition from the hydroxylamine/$FeCl_3$ solution.

We also find that the solution pH plays an important role in determining the outcome of particle deposition on fully hydroxylated SiO_2 surfaces. As shown in Figure 5, for very low and high pH, pH = 2.3 in Figure 5a (adjusted by NH_4OH addition to the solution) and pH = 10 in Figure 5b (adjusted by HCl addition to the solution), no appreciable nanoparticle deposition is observed on the SiO_2 substrates after soaking for 2 min. The optimum pH for particle deposition on these substrates is ~5.

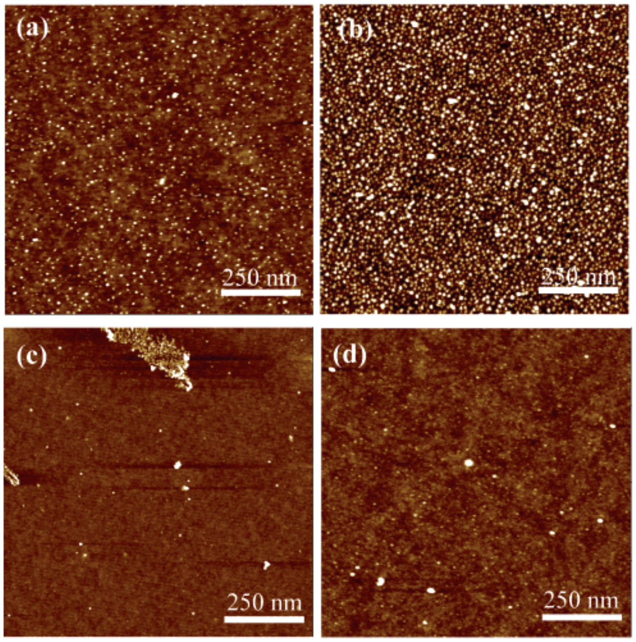

Figure 4. AFM images of hydroxylated SiO_2 surfaces after soaking for (a) 10 s and (b) 5 min respectively in the hydroxylaime/$FeCl_3$ solution. (c) An AFM image showing no systematic particle formation on a SiO_2 substrate without hydroxylamine in the solution. (d) An AFM image showing less particle deposition on a SiO_2 substrate after removal of surface hydroxyl group by high-temperature annealing.

The phenomenon of highly efficient deposition of iron-containing nanoparticles on SiO_2 from the mixed hydroxylamine and $FeCl_3$ solution is interesting. Surveying the literature, we find that hydroxylamine has been used previously to reduce Au^{3+} to Au for deposition onto premade colloidal Au nanoparticles (2−15 nm) and thus for particle enlargement.[15] Brown et al. reported the size increase of Au nanoparticles (either suspended in solution or placed on surfaces) exposed to mixed Au^{3+} and hydroxylamine solutions, and found that while hydroxylamine is efficient in enlarging preformed nanoparticles, it does not lead to nucleation of new Au nanoparticles from the Au^{3+} solution,[15] despite that this is a thermodynamically favored process.[19]

Our current system involves nucleation and growth of nanoparticles on surfaces with hydroxylamine, $FeCl_3$, surface hydroxyls, and pH being the important reaction elements. We can rule out the possibility of nanoparticle formation in the bulk solution phase and subsequent deposition on SiO_2. This is based on the result that larger nanoparticles are observed on the substrate after longer time soaking in the freshly mixed hydroxylamine and $FeCl_3$ solution. Also, in another control experiment, we mixed hydroxylamine and $FeCl_3$ for 2 h and then soaked a SiO_2 chip in the solution. Little or no homogeneous deposition of particles was observed on the substrate. At the present time, however, we do not have a full understanding of the surface-mediated reaction steps involved in our process. We have performed XPS studies of the substrates right after nanoparticle deposition by soaking in the hydroxylamine/$FeCl_3$ solution. Unfortunately, the Fe signal is too weak for identifying the oxidation state of the Fe-containing particles on the surface.

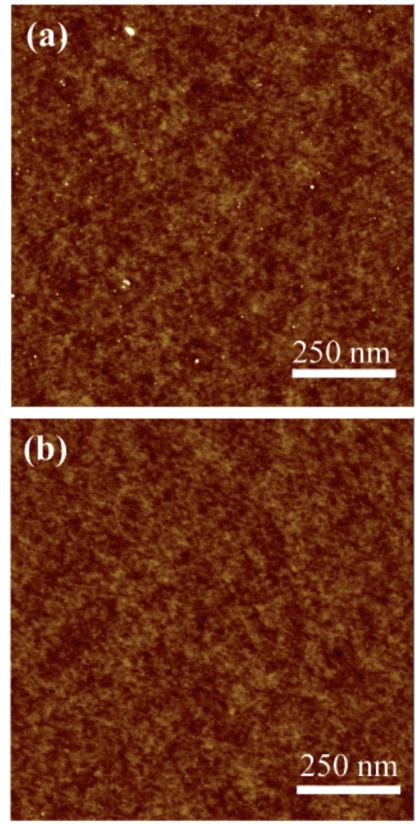

Figure 5. AFM images of hydroxylated SiO_2 surfaces after soaking in hydroxylamine/$FeCl_3$ solution for 2 min, the solution pH is (a) 2.3 and (b) 10, respectively.

Therefore, we cannot definitively assign the nanoparticles to fully reduced Fe nanoparticles. In the literature, little is known about the chemistry between hydroxylamine and $FeCl_3$ on surfaces. Bengtsson et al. studied reactions between hydroxylamine and Fe(III) in solution, especially when the concentration of hydroxylamine is much higher than that of Fe(III), and identified the following solution phase reactions:[20]

$$Fe^{3+} + NH_2OH \leftrightharpoons Fe(NH_2OH)^{3+}$$

$$Fe(NH_2OH)^{3+} \leftrightharpoons Fe^{2+} + H_2NO^{\bullet} + H^+$$

$$2H_2NO^{\bullet} \rightarrow N_2 + 2H_2O$$

The authors did not report the formation of any colloids or particles in the solution. This combined with the results from our control experiments with various types of SiO_2 substrates suggest that the iron-containing nanocluster deposition in our system involves the participation of surface hydroxyl groups. Nevertheless, more systematic investigation is required to understand this chemistry. Instead of speculation on the reaction mechanisms here, we leave this topic for future exploration.

With the hydroxylamine assisted catalyst deposition method, we have carried out catalytic patterning, patterned growth of SWNTs, and integration for nanotube electronic devices. Previously, these were done using alumina-powder

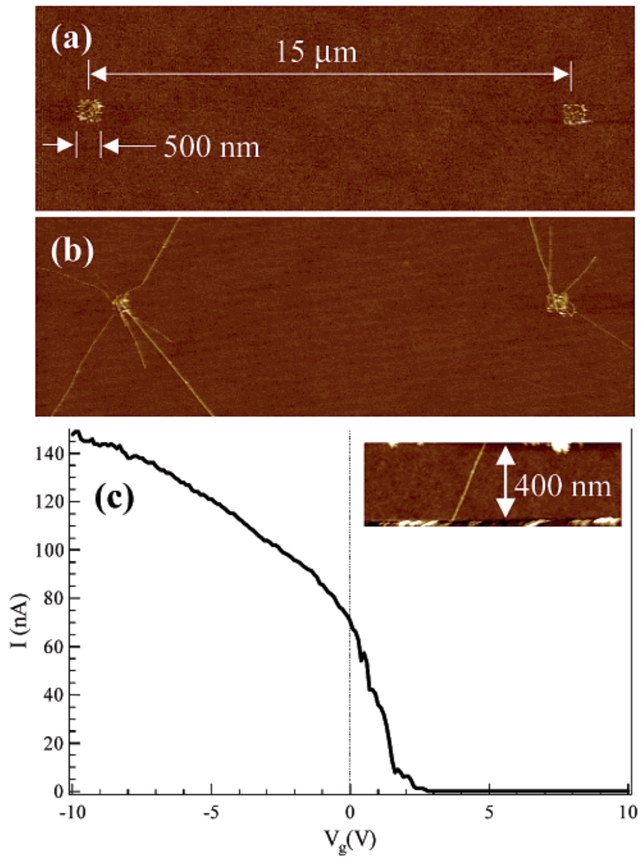

Figure 6. (a) An AFM image of two patterned catalyst islands ($0.5 \times 0.5\ \mu m^2$) on SiO_2 containing iron oxide nanoparticles derived from hydroxylamine assisted deposition. (b) An AFM image showing SWNTs grown from the catalyst islands and clean catalyst regions after growth. (c) Source-drain current (I) vs back-gate voltage (V_g) for a SWNT-FET fabricated on a nanotube grown from an island. Source-drain bias voltage = 100 mV. The inset shows an AFM image of the actual device with a 400 nm long SWNT between electrodes (at the top and bottom of the image).

supported catalysts.[2] With the mound-like alumina support particles left in the patterned regions after CVD growth, however, the catalyst regions on the substrate were not clean and caused problems in sample characterization by, for example, AFM. Here, we patterned $0.5 \times 0.5\ \mu m^2$ wells on a poly(methyl methacrylate) (PMMA) film spun on a SiO_2 substrate by using electron beam lithography,[2] and then soaked the sample in the hydroxylamine/$FeCl_3$ solution for 5 min for nanoparticle deposition. After lift-off of the PMMA film and calcination, we observed a submonolayer of $\sim$2 nm tall Fe_2O_3 nanoparticles well confined inside the $0.5 \times 0.5\ \mu m^2$ patterned regions (Figure 6a). CVD synthesis with such a substrate afforded SWNTs emanating only from these catalytic sites (Figure 6b) that remained smooth, clean, free of large particles, and can be well imaged by AFM. By placing Ti/Au electrodes around the catalyst islands in arrayed fashion, we were able to obtain a high yield of clean nanotube electrical devices (consisting of source S, drain D, and Si back-gate). Figure 6c inset shows an AFM image of a SWNT-FET with 400 nm length between the S−D electrodes. The semiconducting nanotube exhibits typical p-type FET characteristics (Figure 6c).[21]

Conclusion. We have described hydroxylamine assisted deposition of catalyst nanoparticles on SiO_2 substrates from aqueous Fe(III) solutions. The method is very easy and can produce near-monolayer iron oxide catalytic nanoparticles for the synthesis of clean SWNT films on substrates. It also allows for catalytic patterning of substrates at the submicron scale, patterned SWNT growth that retains surface cleanliness, and facile device integration. The optimum deposition condition has been identified through a series of control experiments. However, the detailed chemistry involved in the nanoparticle deposition remains elusive. The simple and efficient hydroxylamine assisted particle deposition offers new opportunities in catalyst patterning at the <100 nm scale, large area patterning via chemical group patterning on substrates, and high-density arrays of clean nanotube devices.

Acknowledgment. We are grateful to Professors Daniel Stack and Christopher Chidsey for discussions about the hydroxylamine/$FeCl_3$ aqueous chemistry. This work is supported by the Packard Foundation, Agilent Technologies, the Sloan Foundation, a Terman Fellowship, and a Camile Dreyfus Teacher-Scholar Fellowship.

References

(1) Dai, H. In *Carbon Nanotubes*; Dresselhaus, M. S., Dresselhaus, G., Avouris, Ph., Eds.; Springer: Berlin, 2001; Vol. 80, pp 29−53.
(2) Kong, J.; Soh, H.; Cassell, A.; Quate, C. F.; Dai, H. *Nature* **1998**, *395*, 878−881.
(3) Cassell, A.; Franklin, N.; Tombler, T.; Chan, E.; Han, J.; Dai, H. *J. Am. Chem. Soc.* **1999**, *121*, 7975−7976.
(4) Zhang, Y.; Chan, A.; Cao, J.; Wang, Q.; Kim, W.; Li, Y.; Morris, N.; Yenilmez, E.; Kong, J.; Dai, H. *Appl. Phys. Lett.* **2001**, *79*, 3155−3157.
(5) Joselevich, E.; Lieber, C. M. *Nano Lett.* **2002**, *2*, 1137−1141.
(6) Ural, A.; Li, Y.; Dai, H. *Appl. Phys. Lett.* **2002**, *81*, 3464−3466.
(7) Soh, H.; Quate, C.; Morpurgo, A.; Marcus, C.; Kong, J.; Dai, H. *Appl. Phys. Lett.* **1999**, *75*, 627−629.
(8) Tombler, T.; Zhou, C.; Alexeyev, L.; Kong, J.; Dai, H.; Liu, L.; Jayanthi, C.; Tang, M.; Wu, S. Y. *Nature* **2000**, *405*, 769−772.
(9) Kong, J.; Franklin, N.; Zhou, C.; Chapline, M.; Peng, S.; Cho, K.; Dai, H. *Science* **2000**, *287*, 622−625.
(10) Zhou, C.; Kong, J.; Dai, H. *Appl. Phys. Lett.* **2000**, *76*, 1597−1599.
(11) Li, Y.; Kim, W.; Zhang, Y.; Rolandi, M.; Wang, D.; Dai, H. *J. Phys. Chem. B* **2001**, *105*, 11424−11431.
(12) Cheung, C.; Kurtz, A.; Park, H.; Lieber, C. *J. Phys. Chem. B* **2002**, *106*, 2429−2433.
(13) Choi, H. C.; Kim, W.; Wang, D.; Dai, H. *J. Phys. Chem. B* **2002**, *106*, 12361−12365.
(14) Kim, W.; Choi, H. C.; Shim, M.; Li, Y.; Wang, D.; Dai, H. *Nano Lett.* **2002**, *2*, 703−708.
(15) Brown, K. R.; Natan, M. J. *Langmuir* **1998**, *14*, 726−728.
(16) Zhang, Y.; Li, Y.; Kim, W.; Wang, D.; Dai, H. *Appl. Phys. A* **2002**, *74*, 325−328.
(17) Jorio, A.; Saito, R.; Hafner, J. H.; Lieber, C. M.; Hunter, M.; McClure, T.; Dresselhaus, G.; Dresselhaus, M. S. *Phys. Rev. Lett.* **2001**, *86*, 1118−1121.
(18) Hair, M. L. *Infrared Spectroscopy in Surface Chemistry*; Marcel Dekker: New York, 1967.
(19) The reduction potential of $AuCl_4^-$ is +1.002 V (vs NHE) and $E_{1/2}$ of NH_2OH is −0.4 V (vs NHE). Reduction potential of Fe(III) to Fe(II) is +0.771 and Fe(II) to Fe(0) is −0.447 V (vs NHE). See Bard, A. J., Ed. *Encyclopedia of Electrochemistry of the Elements*; Marcel Dekker: New York, 1975; Vols. 4 and 8.
(20) Bengtsson, G.; Froneus, S.; Bengtsson-Kloo, L. *J. Chem. Soc., Dalton Trans.* **2002**, 2548−2552.
(21) Tans, S.; Verschueren, A.; Dekker, C. *Nature* **1998**, *393*, 49−52.

NL025876D